Protein Science (1994), *3*:1362–1373. Cambridge University Press. Printed in the USA.

Interactions between human defensins and lipid bilayers: Evidence for formation of multimeric pores

WILLIAM C. WIMLEY,[1] MICHAEL E. SELSTED,[2] AND STEPHEN H. WHITE[1]

[1] Department of Physiology and Biophysics, University of California, Irvine, California 92717-4560
[2] Department of Pathology, University of California, Irvine, California 92717-4800

(RECEIVED April 8, 1994; ACCEPTED June 17, 1994)

Abstract

Defensins comprise a family of broad-spectrum antimicrobial peptides that are stored in the cytoplasmic granules of mammalian neutrophils and Paneth cells of the small intestine. Neutrophil defensins are known to permeabilize cell membranes of susceptible microorganisms, but the mechanism of permeabilization is uncertain. We report here the results of an investigation of the mechanism by which HNP-2, one of 4 human neutrophil defensins, permeabilizes large unilamellar vesicles formed from the anionic lipid palmitoyloleoylphosphatidylglycerol (POPG). As observed by others, we find that HNP-2 (net charge = +3) cannot bind to vesicles formed from neutral lipids. The binding of HNP-2 to vesicles containing varying amounts of POPG and neutral (zwitterionic) palmitoyloleoylphosphatidylcholine (POPC) demonstrates that binding is initiated through electrostatic interactions. Because vesicle aggregation and fusion can confound studies of the interaction of HNP-2 with vesicles, those processes were explored systematically by varying the concentrations of vesicles and HNP-2, and the POPG:POPC ratio. Vesicles (300 μM POPG) readily aggregated at HNP-2 concentrations above 1 μM, but no mixing of vesicle contents could be detected for concentrations as high as 2 μM despite the fact that intervesicular lipid mixing could be demonstrated. This indicates that if fusion of vesicles occurs, it is hemi-fusion, in which only the outer monolayers mix at bilayer contact sites. Under conditions of limited aggregation and intervesicular lipid mixing, the fractional leakage of small solutes is a sigmoidal function of peptide concentration. For 300 μM POPG vesicles, 50% of entrapped solute is released by 0.7 μM HNP-2. We introduce a simple method for determining whether leakage from vesicles is graded or all-or-none. We show by means of this fluorescence "requenching" method that native HNP-2 induces vesicle leakage in an all-or-none manner, whereas reduced HNP-2 induces partial, or graded, leakage of vesicle contents. At HNP-2 concentrations that release 100% of small (~400 Da) markers, a fluorescent dextran of 4,400 Da is partially retained in the vesicles, and a 18,900-Da dextran is mostly retained. These results suggest that HNP-2 can form pores that have a maximum diameter of approximately 25 Å. A speculative multimeric model of the pore is presented based on these results and on the crystal structure of a human defensin.

Keywords: antimicrobial peptides; fluorescence quenching assays; human defensin HNP-2; large unilamellar vesicles (LUV); peptide–bilayer interactions; vesicle fusion; vesicle permeabilization

Reprint requests to: Stephen H. White, Department of Physiology and Biophysics, University of California, Irvine, California 92717-4560; e-mail: shwhite@uci.edu.

Abbreviations: POPG, palmitoyloleoylphosphatidylglycerol; POPC, palmitoyloleoylphosphatidylcholine; LUV, extruded unilamellar vesicles of 100 nm diameter; ANTS, 8-aminonaphthalene-1,3,6 trisulfonic acid; DPX, *p*-xylene-bis-pyridinium bromide; HNP, human neutrophil peptide; NP, rabbit neutrophil peptide; FD-4, fluorescein isothiocyanate-labeled dextran, molecular weight 4,400 Da; FD-20, fluorescein isothiocyanate-labeled dextran, molecular weight 18,900 Da; NBD-PE, 7-nitro-benzoxadiazole phosphatidylethanolamine; rho-PE, lissamine rhodamine phosphatidylethanolamine; rHNP-2, reduced HNP-2; HEPES, *N*-2-hydroxyethylpiperazine-*N'*-2-ethanesulfonic acid; DPPC, dipalmitoylphosphatidylcholine; DOPS, dioleoylphosphatidylserine; RP-HPLC, reverse-phase HPLC; IEX-HPLC, ion exchange HPLC; ex, excitation; em, emission.

A large number of natural antibiotics, as well as venoms and toxins, express their activity through catastrophic increases in cell membrane permeability. Examples of natural membrane-permeabilizing polypeptides, many of which have in vitro antimicrobial and in vivo antibiotic activity, have been found in mammals (Lee et al., 1989; Diamond et al., 1991; Lehrer et al., 1991; Kagan et al., 1992), amphibians (Cruciani et al., 1992), fish (Shai et al., 1988), insects (Lambert et al., 1989; Cociancich et al., 1993a, 1993b), invertebrates (Mangel et al., 1992; Ohta et al., 1992), and prokaryotes (LaLonde et al., 1989; Pattus et al., 1990; Leippe et al., 1992). Among the mammalian antibiotic peptides are the defensins, which are a family of small (M_r = 3,500–4,000) cationic disulfide-stabilized peptides that play an important role in mammalian host defense. Several

structurally similar defensin species are generally present in each animal species. Defensins have been isolated from the cytoplasmic granules of human (Selsted et al., 1985b; Wilde et al., 1989), rat (Eisenhauer et al., 1989), rabbit (Selsted et al., 1985a), and guinea pig (Selsted & Harwig, 1987) neutrophils. These neutrophil defensins are stored in azurophil granules and are used intracellularly to kill phagocytosed microbes. Another family of defensins (enteric defensins), which probably acts extracellularly, is secreted into the small intestine of the mouse (Selsted et al., 1992), rat (Wang et al., 1993), and human (Jones & Bevins, 1992, 1993). A distinct family of 13 defensin-like peptides, called β-defensins, is present in bovine neutrophil granules (Selsted et al., 1993) and in the bovine trachea (Diamond et al., 1991). Structurally similar antimicrobial peptides are also found in the lymph of insects (Cociancich, 1993a, 1993b).

Defensins are active against a wide variety of microbes, including gram-positive and negative bacteria, fungi, and enveloped (but not naked) viruses (Lehrer et al., 1991), and under some conditions they are cytotoxic to eukaryotic cells (Lichtenstein et al., 1986). Defensins sequentially permeabilize the outer and inner membranes of *Escherichia coli*, with cell death occurring concomitantly with inner-membrane disruption (Lehrer et al., 1989). Molecules such as K^+ and disaccharides are released from bacteria in the presence of defensins (Lehrer et al., 1989). Unenergized cells, such as those exposed to uncoupling agents, are protected against defensins (Lehrer et al., 1989). These observations suggest that cell membrane permeabilization is the main source of defensin activity in vivo. This is supported by the observations that defensins form voltage-dependent ion channels in planar bilayers (Kagan et al., 1990) and induce lysis of small sonicated lipid vesicles (Fujii et al., 1993). The work presented here investigates the mechanism of the permeabilization of large unilamellar vesicles by the human defensin HNP-2.

Mature neutrophil defensins are 29–34 amino acids in length, have 6 cysteines, and characteristically have a high content of arginine (4–10 per molecule). The primary sequences of 15 neutrophil defensins have been determined. As can be seen in Figure 1, there are 10 highly conserved residues, which include the 6 cysteines, a Glu/Arg ion pair, and 2 glycines. One of the glycines (G24) is part of a turn and the other (G18) is part of the dimer interface, based upon the X-ray crystallographic structure of HNP-3 (Hill et al., 1991). The 3-dimensional solution (2-dimensional NMR) structures of the human defensin HNP-1, rabbit NP-1, and rabbit NP-5 are very similar to the HNP-3 structure (Pardi et al., 1988, 1992). The structural models show that defensins are compact, globular proteins composed mainly of 3-stranded anti-parallel β-sheet without α-helices. The 3 conserved disulfide bonds per molecule impart a high degree of structural rigidity, based on NMR (Pardi et al., 1988, 1992), circular dichroism (Fujii et al., 1993), and fluorescence spectroscopy (Fujii et al., 1993) measurements. HNP-3 in crystals exists as tight homodimers (Hill et al., 1991), and HNP-1 appears to form dimers or higher multimers in solution (Pardi et al., 1988, 1992). The rabbit defensins NP-1 and NP-5 are apparently monomeric in solution (Pardi et al., 1988, 1992), but the strict conservation of glycine G18 in all of the defensins suggests that dimerization may be generally important for the activity of defensins (Hill et al., 1991).

The HNP-3 dimer has the shape of a basket that is partially flattened at the top, as shown in Figure 2 and Kinemage 1. The bottom of the basket is hydrophobic, whereas the top contains

Defensin	5	10	15	20	25	30
HNP-1	ACYCR	IPAC	IAGER	RYGTC	IYQGR	LWAFC C
HNP-2	CYCR	IPAC	IAGER	RYGTC	IYQGR	LWAFC C
HNP-3	DCYCR	IPAC	IAGER	RYGTC	IYQGR	LWAFC C
HNP-4	VCSCR	LVFC	RRTEL	RVGNC	LIGGV	SFTYC CTRV
GPNP	RRCICT	TRTC	RFPYR	RLGTC	IFQNR	VYTFC C
NP-1	VVCACR	RALC	LPRER	RAGFC	RIRGR	IHPLC CRR
NP-2	VVCACR	RALC	LPLER	RAGFC	RIRGR	IHPLC CRR
NP-3A	GICACR	RRFC	PNSER	FSGYC	RVNGA	RYVRC CSRR
NP-3B	GRCVCRKQLLC	SYRER	RIGDC	KIRGV	RFPFC CPR	
NP-4	VSCTCR	RFSC	GFGER	ASGSC	TVNGV	RHTLC CRR
NP-5	VFCTCR	GFLC	GSGER	ASGSC	TINGV	RHTLC CRR
RatNP-1	VTCYCR	RTRC	GFRER	LSGAC	GYRGR	IYRLC CR
RatNP-2	VTCYCR	STRC	GFRER	LSGAC	GYRGR	IYRLC CR
RatNP-3	CSCR	TSSC	RFGER	LSGAC	RLNGR	IYRLC C
RatNP-4	ACYCR	IGAC	VSGER	LTGAC	GLNGR	IYRLC CR

Fig. 1. Sequences of neutrophil defensins. Conserved residues are shown in bold and the 6 conserved cysteine residues are also underlined. The connectivities of the 6 cysteine residues are: 1–6, 2–4, 3–5. The sequences are for human HNP-1, -2, -3 (Selsted et al., 1985b) and HNP-4 (Wilde et al., 1989), guinea pig GPNP (Selsted & Harwig, 1987), rabbit NP-1–NP-5 (Selsted et al., 1985a), and rat RatNP-1–RatNP-4 (Eisenhauer et al., 1989).

polar side chains as well as the N- and C-termini of both monomers. The methylene groups of some of the 8 arginines contribute to the hydrophobic surface, while the charged guanidine ends form a ring around the dimer (Hill et al., 1991). This "structural amphiphilicity" of the HNP-3 dimer led Hill et al. (1991) to propose 3 possible models for the mechanism of defensin activity: (1) detergent-like monomeric dimers, (2) a dimer of dimers with a solvent channel between, or (3) an annulus of defensin dimers that constitute a large pore. The evidence we present here supports the large-pore model.

Results

The main goal of our investigation of the interactions of defensin HNP-2 with large unilamellar vesicles was to establish the mechanism by which defensins permeabilize the vesicles. However, Fujii et al. (1993) reported that defensins induce simulta-

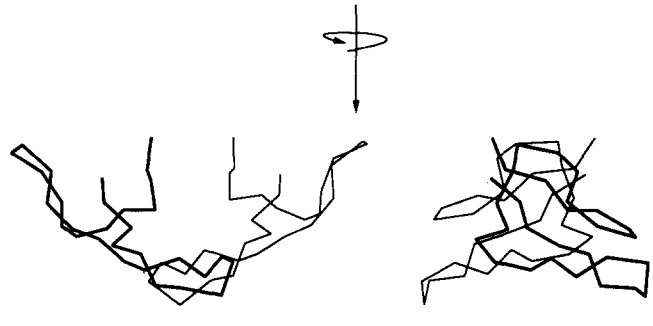

Fig. 2. Two views of the α-carbon backbone of the HNP-3 dimer from the crystal structure (Hill et al., 1991). These 2 views differ by a 90° rotation around the indicated axis to illustrate the basketlike shape of the dimer. One of the subunits is drawn as a bold line for clarity. The flattened basket top, containing the N- and C-termini of the peptide, is at the top of the image and the broad basket bottom, containing the "hydrophobic base," is at the bottom.

neous aggregation, fusion, and lysis of small sonicated vesicles formed from DPPC and DOPS. Because such effects complicate studies of permeabilization mechanisms, our first objective was to develop a more stable vesicle preparation that could be used to distinguish the effects of aggregation and fusion from changes in bilayer permeability. We found that vesicles formed from mixtures of neutral POPC and negatively charged POPG constituted such a system. By carefully controlling the experimental conditions, we were able to examine defensin-induced release of molecules of different sizes under conditions of limited aggregation and fusion. We wish to emphasize, however, that aggregation occurs to some extent no matter what the experimental conditions are. Although we examined permeabilization under conditions that permit us to be confident about our conclusions, the defensin/lipid/aqueous system is, grossly speaking, a 3-phase system comprised of defensin in solution, defensin/lipid aggregates, and vesicle-bound defensin. This means that one cannot be entirely certain of the absolute concentration of defensin in any of the phases. The experiments proceeded in 4 steps by studying first the binding of HNP-2 to vesicles and then its induction of aggregation, fusion, and permeabilization. Large unilamellar vesicles with a nominal diameter of 0.1 μm were used in the experiments. The LUV concentrations reported below refer the total concentration of lipid in the solution.

Binding of HNP-2 to lipid vesicles

Equilibrium dialysis and reverse-phase HPLC (Wimley & White, 1993a) show that the binding of HNP-2 to LUV composed of zwitterionic POPC and anionic POPG is a sigmoidal function of the mole % of anionic lipid (Fig. 3) and that HNP-2 binds to vesicles only when POPG is present, as expected for electrostatic interactions (Kim et al., 1991). The experiments were carried out by placing 14 μM HNP-2 in one half-cell and either 1 mM or 10 mM of POPC/POPG LUV in the other. The binding to 100% POPG (10 mM vesicles) saturates with approximately 90% of the peptide bound and 10% free in solution so that free and bound defensins are probably in equilibrium under these conditions. Saturation is also observed for 1 mM 100% POPG vesicles, but in that case extensive aggregation occurs. These results emphasize that the defensin is found in at least 3 different phases.

The complexity and heterogeneity of bilayers cause most peptide–bilayer interactions to arise from a combination of hydrophobic, electrostatic, and so-called "bilayer" effects (Wimley & White, 1993b; White & Wimley, 1994). The multiple effects of defensins on bilayers (see below) suggest that this is true for defensins as well. However, our binding experiments indicate that electrostatic interactions are a prerequisite for the occurrence of other interactions.

Formation of large peptide/lipid aggregates

Aggregate formation was assayed in the binding experiments by measuring the fraction of peptide in the lipid-containing dialysis half-cell that was pelletted by mild centrifugation (Fig. 3). Large peptide/lipid aggregates formed only when HNP-2 was incubated with 1 mM vesicles containing greater than 40% POPG. Large aggregate formation was not observed at 10 mM lipid under any circumstances (0–100% POPG) or at 1 mM lipid at low POPG content. These observations suggest that POPG vesicles are aggregated by HNP-2 electrostatically. The composition of the large aggregates can be inferred from Figure 4, which shows the composition of the aggregates as a function of the mole ratio of POPG to HNP-2. Virtually none of the lipid is found in the aggregates until the POPG:HNP-2 drops below

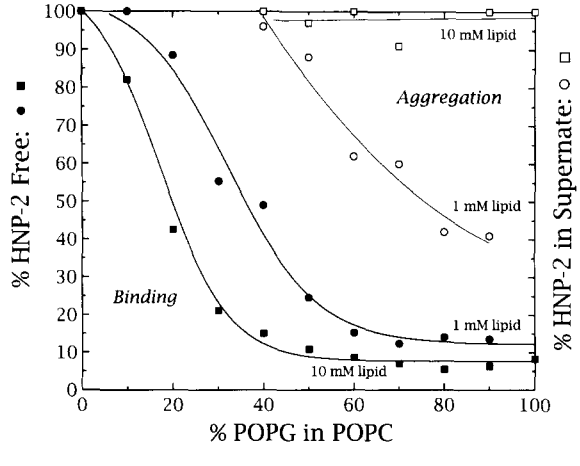

Fig. 3. Peptide binding and vesicle aggregation in mixtures of HNP-2 and POPC/POPG vesicles. Binding (filled symbols) was assayed by equilibrium dialysis and HPLC (Wimley & White, 1993a). The fraction of peptide in the form of large peptide–lipid aggregates in the lipid half-cell (open symbols) was assayed by HPLC and centrifugation (see text). Dialysis experiments were begun with 1 mM (circles) or 10 mM (squares) vesicles containing mixtures of POPC and POPG in 1 cell half and 14.5 μM HNP-2 in the other. The lower curves are best-fit sigmoidal curves demonstrating that binding, and probably aggregation, is primarily by electrostatic interactions.

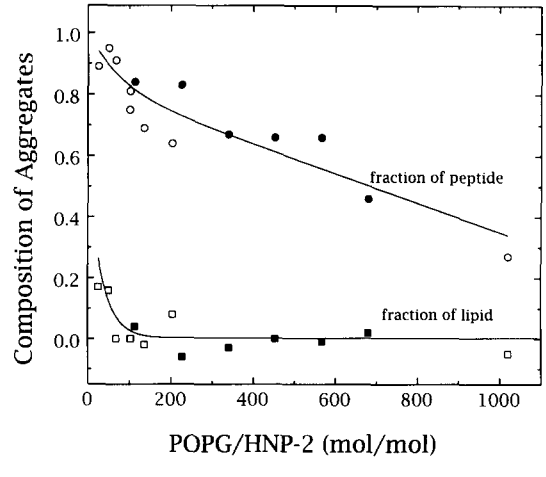

Fig. 4. Composition of large peptide/lipid aggregates. Lipid and peptide were mixed and incubated for 30 min. The fractions of lipid (squares) and peptide (circles) in the large aggregates were determined using HPLC and fluorescence following centrifugation (see text). Experiments were performed either by adding HNP-2 to 300 μM POPG vesicles (open symbols) or by adding POPG vesicles to 1.7 μM HNP-2 (filled symbols). The combined data from 2 experiments are plotted together with the POPG/HNP-2 ratio as the common abscissa. The aggregates are highly enriched in peptide and, in most experiments, contain a negligible fraction of the total lipid.

100:1, at which point almost all of the HNP-2 is found in the pellet. The measurements of the permeabilization of vesicles by HNP-2 were carried out a POPG:HNP-2 ratios of greater than 100:1 so that the total amount of lipid involved in aggregation was negligible.

We infer from Figure 4 that the composition of the large aggregates is approximately 10 lipids per HNP-2. POPG and defensin dimers have approximate cross-sectional surface areas of ~70 and ~300–400 Å^2, respectively. Close-packed defensins bound between apposed bilayers could cover a maximum of ~10 lipids/peptide, suggesting that the large aggregates may be composed of tightly aggregated bilayers separated by a layer of close-packed defensins. This behavior has been observed for the Ca^{2+}-induced aggregation of phosphatidylserine bilayers (Feigenson, 1989). Alternatively, the defensins could be incorporated into a lamellar structure with defensins surrounded by, at most, 1 layer of lipids, as suggested by small-angle X-ray diffraction studies on oriented multilayers composed of mixtures of HNP-2 and dioleoylphosphatidylcholine (Wimley et al., 1993). We found that mixtures containing up to 10 mol % HNP-2 give well-ordered lamellar diffraction patterns and that the lamellar repeat spacing decreases linearly from 49.5 ± 0.3 Å at 100% DOPC to 44.9 ± 0.8 Å with 10 mol % HNP-2. These results suggest that the peptide is incorporated into the bilayers (not phase-separated) under the diffraction conditions of low hydration (5.4 waters/lipid).

Aggregation of POPG vesicles by HNP-2 was also assayed by absorbance spectroscopy (Fig. 5). In the presence of 300 μM POPG vesicles, the onset of aggregation appears to begin at approximately 0.9 μM HNP-2, where, at most, 1% of the lipid bilayer charge has been neutralized. This suggests that bound defensins are probably recruited by diffusion and concentrated in regions of close bilayer contact because aggregation can only occur when the surface charge in the contact area is neutralized (Leventis et al., 1986).

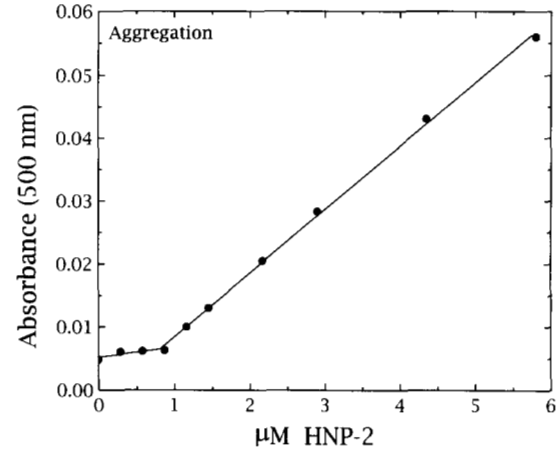

Fig. 5. Aggregation of POPG LUV caused by HNP-2. HNP-2-induced aggregation was assayed using optical absorbance of 300 μM POPG LUV after incubation for 30 min with HNP-2. The optical absorbance of the solution was measured at a wavelength of 500 nm in an unstirred 1 × 1-cm cuvette. The onset of aggregation occurs at approximately 1 μM HNP-2.

Fusion processes: Intervesicular lipid mixing

A possible explanation of vesicle permeabilization induced by HNP-2 is that leakage occurs incidental to vesicle fusion events caused by local destabilization of the LUV bilayers. A careful examination of the nature of LUV interactions induced by HNP-2 was therefore necessary. The possible interactions include (1) transient associations, which result in exchange of lipids between vesicles, (2) hemi-fusion involving stable associations of vesicles in which the outer monolayers fuse and thereby exchange lipids, and (3) complete fusion, which results in (a) the mixing of the lipids of the fused bilayers and (b) the mixing of the contents of the vesicles. The first 2 interactions are difficult to distinguish from one another and we made no attempt to do so. We therefore refer to processes involving the exchange of lipids between vesicles in the absence of the mixing of contents as "intervesicular lipid mixing."

Lipid mixing was assayed by the NBD-PE/rho-PE fluorescence quenching assay (Struck et al., 1981). NBD-PE and rho-PE present at 1 mol % in POPG LUV have low fluorescence because of the quenching of rho-PE by NBD-PE. The addition of HNP-2 to a solution of labeled LUV diluted 10-fold with unlabeled LUV resulted in a large increase in fluorescence (Fig. 6). This means that the bilayer concentrations of NBD-PE and rho-PE have been decreased by dilution with POPG due to HNP-2-induced lipid mixing. This conclusion is further supported by the fact that the apparent extent of mixing increases with peptide concentration (Fig. 7). Note in Figure 7, however, that the fractional mixing never exceeds about 50% under the most optimal conditions of high HNP-2 concentrations (~5 μM) and the use of osmotic stress to enhance fusion (Woodbury & Hall, 1988). We were surprised to observe that lipid mixing was reduced under low-salt conditions, which should enhance peptide binding and vesicle aggregation. Together, these results indicate that lipid mixing is relatively inefficient in this system and par-

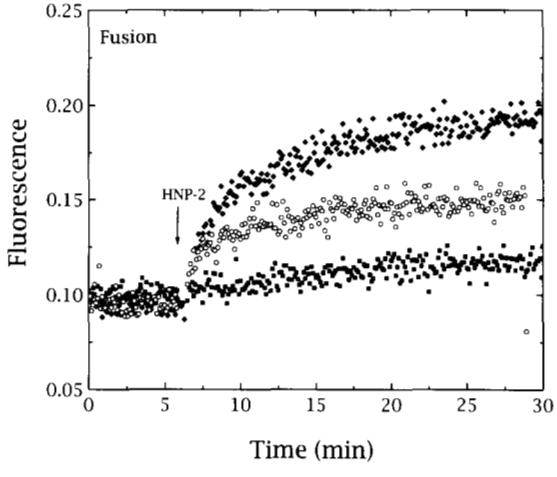

Fig. 6. Kinetics of POPG intervesicular lipid mixing. Lipid mixing of vesicles was assayed by the NBD-PE/rho-PE probe dilution assay (see text). Initially, POPG vesicles containing 1% each NBD-PE and rho-PE were mixed with a 10-fold excess of unlabeled vesicles. HNP-2 was added at approximately 8 min and the fluorescence monitored. Total lipid concentration was 300 μM with peptide concentrations of (top to bottom in figure) 5.3, 1.7, and 0.4 μM HNP-2. HNP-2 causes an exponential increase in fluorescence toward a plateau level that increases with the HNP-2 concentration.

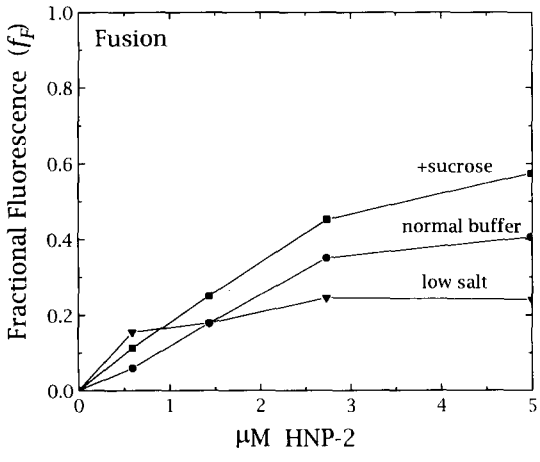

Fig. 7. Fractional fluorescence change (f_F) due to HNP-2-induced intervesicular lipid mixing between POPG LUV. Fractional fluorescence is the increase in NBD-PE fluorescence, due to lipid mixing, relative to the maximum possible increase, calculated assuming complete dilution of both probes (see text). Normal buffer: 50 mM KCl, 10 mM HEPES; low-salt buffer: 0 KCl, 10 mM HEPES; +sucrose: osmotically stressed vesicles with normal buffer outside and normal buffer + 200 mM sucrose inside. HNP-2 induces a moderate level of lipid mixing of POPG LUV above ~1 μM HNP-2. Osmotic stress enhances lipid mixing, whereas low salt inhibits it.

ticularly so at the low HNP-2 concentrations (~1 μM) that were found to permeabilize the vesicles (see below). We also examined the effect of reduced HNP-2 and found that it does not induce lipid mixing under the above conditions. This indicates that lipid mixing can only occur when the HNP-2 is in its folded, compact state.

The extent to which the contents of the vesicles were mixed during the lipid-mixing interactions, indicative of complete fusion, was assayed by the method of Ellens et al. (1984). HNP-2 was added to a solution of POPG vesicles containing either the fluorescent dye ANTS or the quencher DPX. If the vesicles fully fuse, then there should be a decrease in ANTS fluorescence as the DPX quenches the ANTS as the vesicle contents mix. However, we could detect no mixing of contents (data not shown) within a limit of approximately 3% fusion. "Leaky" vesicles that are also undergoing fusion will generally show at least a transient decrease in fluorescence during the initial stages of fusion (Ellens et al., 1984), but no such transients were observed. The apparent lack of contents mixing and the limited mixing of bilayer lipids detected with the NBD/rhodamine assay indicates that the defensin-induced fusion of the inherently stable POPG LUV is not a significant issue. If fusion occurs, it is limited to hemi-fusion resulting from the mixing of outer-monolayer lipids at bilayer contact sites (Leventis et al., 1986).

Leakage of vesicle contents

The ANTS-DPX fluorescence quenching system (Ellens et al., 1984) was also used to assess the leakage of vesicle contents induced by HNP-2. In this case, the fluorescent ANTS and the quencher DPX were coencapsulated within POPG LUV so that leakage would be signaled by an increase in ANTS fluorescence due to dilution into the extravesicular space. The maximum fluorescence possible (F_{max}) for the amount of ANTS entrapped was established by lysis of the vesicles with Triton X-100 detergent. In the absence of leakage, a fluorescence $F_{initial} = Q \cdot F_{max}$ is observed, where Q is the quenching factor (typically 0.2). Figure 8 shows that the fluorescence increases exponentially in time to a plateau value (F_{final}) upon the addition of HNP-2 and therefore demonstrates that HNP-2 induces leakage. Superimposed upon the relatively fast leakage is slow leakage that increases linearly in time at a rate of 1-2% per hour. The fractional fluorescence increase, $f_F = (F_{final} - F_{initial})/(F_{max} - F_{initial})$, increases with HNP-2 concentration and reaches values of about 0.95 for high concentrations. Reduced HNP-2 also causes leakage and produces results similar to those shown in Figure 8 (data not shown). The reason for the plateau behavior that results in $f_F < 1$ at intermediate defensin concentrations is not clear. The simplest possibility is that the concentration of HNP-2 that is bound to vesicles and competent to induce leakage passes through a maximum and then decreases as it distributes itself between the vesicle-bound and aggregated forms. Another possibility is that the leakage mechanism itself is transient, as would be observed, for example, if the defensin molecules in the process of reaching a final nonpermeable equilibrium configuration passed through a permeable intermediate state.

The half-times for leakage drop sharply from about 15 min to 2 min as the concentration of HNP-2 increases, as shown in Figure 9, where the half-times, determined from data like those of Figure 8, have been plotted against HNP-2 concentration. The leakage half-times for rHNP-2 (about 1.5 min at 0.1 μM) that are included in Figure 9 show that rHNP-2 is more active than the native HNP-2. This is shown more clearly in Figure 10, where f_F is plotted against defensin concentration for both HNP-2 and rHNP-2 (inset). For native HNP-2, $f_F = 0.5$ occurs at a peptide concentration 0.7 ± 0.2 (SD) μM (18 experiments), whereas for rHNP-2, 50% leakage occurs at 0.07 μM rHNP-2. Fujii et al. (1993) have also observed that reduced human and rabbit defensins are more active than the native forms. The gen-

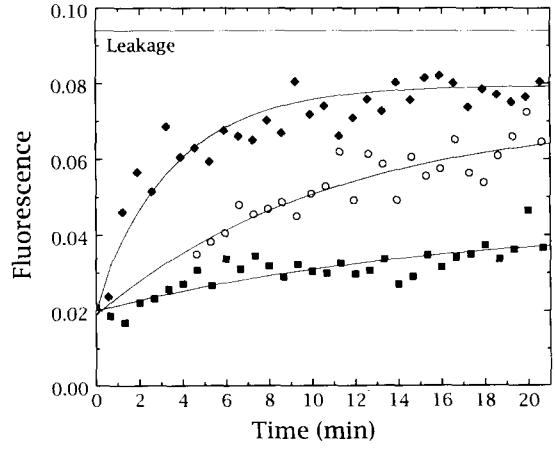

Fig. 8. Kinetics of ANTS leakage from POPG vesicles. Leakage of ANTS and DPX from POPG LUV caused by HNP-2 was assayed by fluorescence (see text). HNP-2 was added to 300 μM POPG vesicles with entrapped ANTS and DPX at time = 0 on these curves. The peptide concentrations shown are (top to bottom) 1.3, 0.7, and 0.3 μM HNP-2. The horizontal line represents the fluorescence intensity of vesicles lysed with Triton X-100. HNP-2 causes an exponential increase in fluorescence toward a plateau level that increases with HNP-2 concentration.

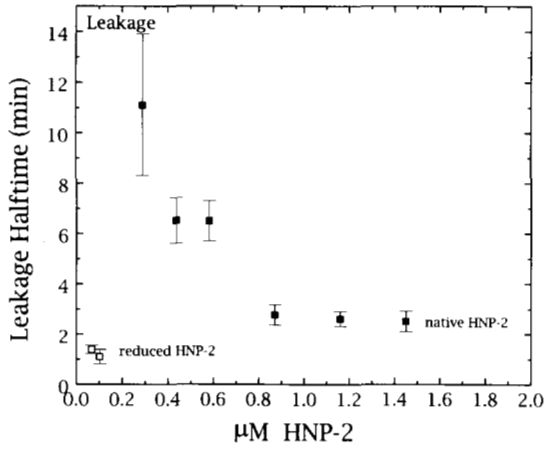

Fig. 9. Rate of leakage of the contents of POPG vesicles induced by native and reduced HNP-2. Half-times were determined by least-squares curve fitting to the kinetic curves (Fig. 8) assuming an exponential approach combined with a slow linear increase (if necessary). The half-time of HNP-2-induced contents leakage rapidly decreases with increasing HNP-2 concentration toward an apparent minimum value of about 2 min.

eral features of defensin-induced leakage described here have also been observed for melittin (Schwarz et al., 1992) and the channel-forming peptide GALA (Parente et al., 1990).

The leakage process

The general image of leakage that emerges from the data above is that it is a transient event(s) that depends upon the conformation and concentration of the defensin. There are 2 ways that leakage could occur. It could be a graded process, in which all of the vesicles release portions of their contents, or it could be all-or-none, in which some fraction of the vesicles lose either all of their contents or none. These 2 possibilities are usually distinguished by determining the level of quenching in vesicle fractions chromatographically separated from external fluorophor after peptide-induced leakage has occurred (Parente et al., 1990; Grant et al., 1992; Ostolaza et al., 1993). Alternately, the quenching can be determined more easily and accurately without separating free and entrapped fluorophor by measuring the overall quenching factor Q_{total} following the incremental addition of DPX quencher to the vesicle/peptide preparation after the fluorescence plateau (Fig. 8) has been reached. This "requenching" procedure, as we describe in the next paragraph, permits one to distinguish the 2 types of leakage and, at the same time, determine the actual fraction of entrapped ANTS released.

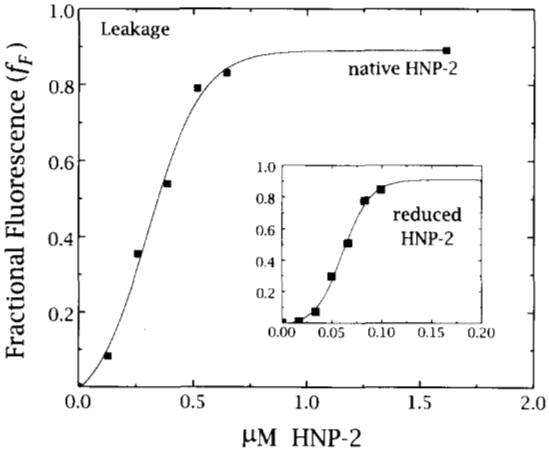

Fig. 10. Fractional change in quenched ANTS fluorescence caused by leakage that is induced by native and reduced HNP-2. Fractional fluorescence (f_F) is the increase in ANTS fluorescence in the plateau region after addition of HNP-2 (see Fig. 8) relative to the fluorescence after lysis of vesicles with 0.2% Triton X-100. Measurements were made approximately 45 min after defensin addition. The full-size plot shows data for native defensins and the **inset** data for reduced (denatured) defensins. Fractional fluorescence is a steep sigmoidal function of HNP-2 concentration. The plots show that rHNP-2 is more active than native HNP-2.

For a given addition of DPX, the total quenched fluorescence observed will be $F_{total} = F_{QO} + F_{QI}$, where F_{QO} is the quenched fluorescence originating from outside the vesicles and F_{QI} is that from within. If there were no quenching, the observed total fluorescence from ANTS inside and outside the vesicles would be $F_{max} = F_{MO} + F_{MI}$. The addition of Triton X-100 to the system causes lysis of the vesicles and dilution of the DPX so that the fluorescence observed in that case will be F_{max}. The quenching outside and inside the vesicles is given, respectively, by $Q_{out} = F_{QO}/F_{MO}$ and $Q_{in} = F_{QI}/F_{MI}$, so that the total quenched fluorescence may be written $F_{total} = Q_{total} \cdot F_{max} = Q_{out} \cdot F_{MO} + Q_{in} \cdot F_{MI}$. The fractions of ANTS outside and inside the vesicles are $f_{out} = F_{MO}/F_{max}$ and $f_{in} = F_{MI}/F_{max}$, and it must be true that $f_{out} + f_{in} = 1$. Therefore, the total quenching will be

$$Q_{total} = Q_{out} \cdot f_{out} + Q_{in} \cdot (1 - f_{out}). \quad (1)$$

We are interested in the behavior of Q_{in} because it reflects the state of the contents of the vesicles. If Q_{in} is independent of the fraction of ANTS that has leaked out, then we conclude that the leakage is all-or-none. If it increases with f_{out}, then we conclude that the leakage is graded. Experimentally, we first lyse defensin-free vesicle-encapsulated ANTS/DPX preparations with Triton X-100, incrementally add DPX, and measure the normalized fluorescence $F_{DPX}/F_{max} = Q_{out}$ in order to obtain a calibration curve for calculating the value of Q_{out} for a particular DPX addition. We then add defensin to an ANTS/DPX vesicle solution and incubate for long enough to reach the plateau level of fluorescence. With this solution, we measure F_{total} as a function of added DPX concentration. After the last addition of DPX, we add Triton X-100 to determine F_{max}. With those measurements and the Q_{out} calibration curve, we plot Q_{total} versus Q_{out} and obtain a linear curve with slope f_{out} and intercept $Q_{in} \cdot (1 - f_{out})$ determined using linear least-squares fitting procedures.

The internal quenching as a function the fraction of ANTS released for HNP-2 and rHNP-2 is shown in Figure 11. The results are unequivocal: rHNP-2 causes graded leakage whereas HNP-2 causes all-or-none leakage. Even after more than 80% of the total entrapped ANTS has been released by native HNP-2, the encapsulated remainder is quenched by an amount indistinguishable from the initial value. All-or-none leakage of vesicle contents, which has been observed for melittin (Schwarz et al., 1992), magainin (Grant et al., 1992), GALA (Parente et al., 1990), and α-hemolysin (Ostolaza et al., 1993), is consistent with

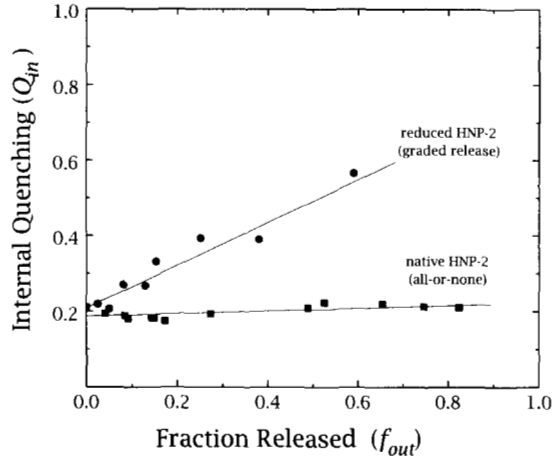

Fig. 11. Plots of internal quenching (Q_{in}) of vesicle contents as a function of the fraction of contents released (f_{out}) for the determination of the mechanism of vesicle leakage. The level of DPX quenching remaining inside the vesicles after incubation with HNP-2 was determined by titrating DPX into vesicle solutions after incubation with increasing concentrations of reduced (circles) or native (squares) HNP-2. The internal quenching level was calculated as described in the text. The initial quenching level was 0.21 before addition of HNP-2. Both f_{out} and Q_{in} have uncertainties of approximately 0.025 (within the diameters of the data points). The data show unambiguously that rHNP-2 causes partial, or graded, release of vesicle contents, whereas native HNP-2 causes all-or-none release of vesicle contents.

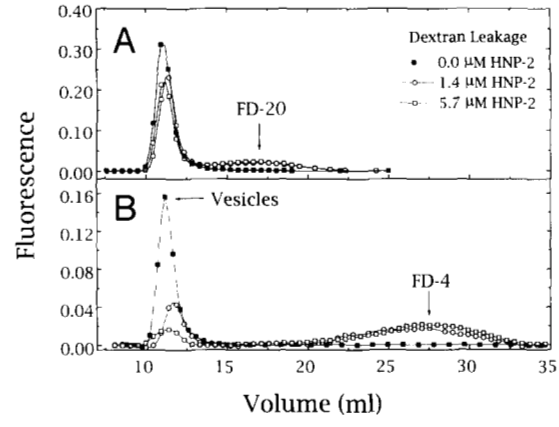

Fig. 12. Leakage of FITC dextrans assayed by gel filtration chromatography. POPG vesicles containing FITC dextrans of 4,400 Da (FD-4) and 18,900 Da (FD-20) were incubated for 2 h with 0, 1.5, and 5.8 μM HNP-2 and then fractionated by gel filtration (see text). Relative concentration of dextrans in each fraction was determined by fluorescence. These experiments demonstrate a sharp dependence of dextran leakage on size (see Table 1).

a threshold phenomenon such as the complete disruption of vesicle structure or the formation of pores. In the latter case, one can suppose that multimeric pores are formed in only those vesicles that have a sufficient number of defensin molecules present for a long enough period for a pore to assemble. The graded leakage induced by reduced defensin suggests some sort of destabilizing effect on all of the vesicles in the system, acting, perhaps, in the manner of a detergent. Fujii et al. (1993) have suggested that the conformational changes they observed for reduced human and rabbit defensins induced amphipathic structures that transiently destabilized bilayers. Consistent with this, we have observed that rHNP-2, unlike the native form, induces leakage in vesicles formed from charge-neutral POPC alone (data not shown).

Mechanism of all-or-none leakage

The 2 possibilities for all-or-none leakage mentioned earlier were gross vesicle destabilization and multimeric pore formation. To distinguish which of these two is the more likely, we examined by gel filtration the leakage of 2 fluorescent dextrans, FD-4 and FD-20, that differ greatly in molecular weight. The data presented in Figure 12 and Table 1 show that 100% of ANTS/DPX (~400 Da), 64% of FD-4 (4,400 Da), and 24% of FD-20 (18,900 Da) are released at 1.4 μM HNP-2. Similar results are observed at 5.7 μM. These observations demonstrate clearly that the all-or-none leakage of ANTS is not due to simple vesicle disruption. Instead, the permeability barrier of the bilayers is disrupted by structures that are large enough to allow the leakage of ANTS/DPX and FD-4, but are too small to allow the release of FD-20.

The bacterial toxin α-hemolysin (Ostolaza et al., 1993) and the amphipathic peptide GALA (Parente et al., 1990) have also been reported to induce all-or-none leakage of ANTS/DPX from large unilamellar vesicles in experiments similar to ours. However, the α-hemolysin-induced leakage of FITC-dextrans was found to be independent of their molecular weight up to 17,200 Da, leading Ostolaza et al. (1993) to conclude that α-hemolysin probably causes all-or-none leakage through a detergent-like disruption of vesicular structure. The GALA peptide, on the other hand, was shown only to release molecules smaller than approximately 800 Da, leading Parente et al. (1990) to conclude that GALA forms pores that are 10–20 Å in diameter.

Discussion

Fujii et al. (1993) reported that the human defensin HNP-1 induced 20–50% fusion of sonicated vesicles of 3:1 DPPC:DOPS. Similarly, we find that native HNP-2 induces intervesicular lipid mixing of POPG LUV (Figs. 6, 7) that reaches a plateau at approximately 40% under iso-osmotic conditions. Lipid mixing is increased by osmotic stress and decreased by low salt concentration. Whereas Fujii et al. (1993) reported that reduced (and *S*-carboxamidomethylated) HNP-1, like native HNP-1, causes 20–50% fusion in 5–10 mM phosphate buffer, we find that rHNP-2 does not cause lipid mixing of POPG LUV. Differences in the model membrane systems used in these experiments probably account for the different experimental observations. Fujii et al. (1993) used sonicated vesicles, which may have been composed of phase-separated domains of gel-phase DPPC and fluid-phase DOPS. Such vesicles are probably unstable, and will have a greater tendency to undergo fusion and lysis (Nicolussi et al., 1982; Wong et al., 1982). As Fujii et al. (1993) pointed out, the cationic and amphipathic nature of both native and reduced defensins may promote fusion and lysis in this system.

In the experiments presented here, we have used inherently more stable large unilamellar vesicles composed of fluid-phase POPG, which will be less likely to undergo spontaneous fusion or lysis. Although native HNP-2 induces intervesicular lipid mix-

Table 1. *Release of markers of various molecular weights by HNP-2*

Compound	Molecular weight	R_h (Å)[a]	Axial ratio[b]	Percent release 1.5 μM HNP-2	Percent release 5.8 μM HNP-2
ANTS/DPX	~400	~6[c]	–	90–100[d]	90–100
FD-4	4,400	18.5[e]	2.2	64[f]	85
FD-20	19,000	29.5[e]	8.5	24	29

[a] Hydrodynamic radius.
[b] Ratio of major axis to minor axis determined by analytical ultracentrifugation (Bohrer et al., 1979).
[c] Estimate based upon the molecular weight and diffusion coefficients of small molecules.
[d] Percent release of ANTS/DPX and FITC dextrans from POPG LUV induced by incubation of 300 μM vesicles with HNP-2. See text.
[e] Hydrodynamic radii of dextrans taken from Bohrer et al. (1979). See text.
[f] Percent dextran released is the average of values from 2 experiments.

ing, no mixing of vesicle contents is detectable. If fusion is occurring, this observation indicates that it must be hemi-fusion, in which only the outer monolayer lipids mix at bilayer contact sites. Hemi-fusion can occur when 2 bilayers are brought into close physical contact (Burgess et al., 1991), but does not always result from vesicle aggregation (Fujii et al., 1993). The electrostatic aggregation of POPG vesicles by HNP-2 could lead to such close contact, and the amphipathic nature of the peptide could lead to the sort of bilayer destabilization that promotes hemi-fusion (Siegel, 1993). The lack of contents mixing also suggests that the defensin-rich vesicle-contact sites are unlikely to contain transmembrane pores and therefore that defensins involved in intervesicular aggregation may not be competent to form pores.

In contrast to classical α-helical channel-forming peptides, such as melittin (Tosteson & Tosteson, 1981), defensins are rigid, compact, globular peptides that are rich in β-sheet, with no α-helices (Pardi et al., 1988, 1992; Hill et al., 1991). Despite the obvious structural differences, defensins have been reported to permeabilize cell membranes in vivo (Lehrer et al., 1989), cause lysis of sonicated lipid vesicles (Fujii et al., 1993), and induce voltage-dependent ion channels in vitro (Kagan et al., 1990). We have found that HNP-2 forms voltage-dependent ion channels in planar bilayers at concentrations as low as 0.3 μM (W.C. Wimley & J. Hall, unpubl. obs.). The bilayer conductance is a steep function of voltage, as has also been reported for rabbit defensin NP-1 by Kagan et al. (1990). This is not surprising because the defensin dimer carries a charge of +6. In the work presented here, we have found that the human defensin HNP-2 causes leakage of entrapped fluorescent dye (ANTS) and its quencher DPX (MW ~400) from POPG LUV. During the leakage process, the vesicles leak either all of their contents or none. HNP-2 induces leakage of a dextran of M_r = 4,400 to a lesser extent than ANTS, but to a greater extent than a dextran of M_r = 18,900.

The contents-leakage experiments were done at HNP-2 concentrations that induced only limited fusion and aggregation (see Figs. 5, 7). Although our data do not allow us to completely rule out the possibility that the defensin-induced vesicle leakage occurs via leaky fusion events, several lines of evidence argue against it. First, HNP-2 does not apparently induce full fusion in this system, but rather only intervesicular lipid mixing that may possibly be due to hemi-fusion. Thus, the large-molecule permeability barrier of the membrane structure in the region of defensin-induced contact and lipid mixing is likely to remain intact. Second, at HNP-2 concentrations that caused 50% of the vesicles to release their contents, the extent of vesicle aggregation is negligible and the extent of "fusion" is less than 10%. At HNP-2 concentrations that caused complete contents release, fusion is less than 20% (Figs. 6, 9). Third, the sharp permeability differences between FD-4 and FD-20 (which are essentially polymeric rods of different lengths; see below) suggest that the leakage path has a rather well-defined size. This would not be expected to be the case for transient structures formed during fusion of fluid-phase bilayers.

Based upon the structural amphiphilicity of the HNP-3 dimer, Hill et al. (1991) proposed 3 possible mechanisms for defensin activity: (1) Single defensin dimers act as a wedge to disrupt the packing of the lipids in the bilayer. In this model, the hydrophobic basket bottom of the HNP-3 dimer is inserted into the hydrocarbon layer of one lipid monolayer while the polar groups of the basket top and the arginine arms maintain contact with the headgroup region and aqueous phase. (2) A dimer of dimers spans the bilayer so that a small solvent channel is formed between them, consistent with the observation of a small solvent channel in the HNP-3 crystal structure through the top of the HNP-3 basket. The channel would be part of the polar interface between 2 dimers and the hydrophobic basket bottoms would face outward toward the bilayer hydrocarbon. (3) An annulus of dimers forms a large central pore. The dimers would also span the bilayer as in model 2, but with a rotated orientation such that the hydrophobic basket bottoms face outward, into the bilayer, while the polar basket tops line the channel.

Our results are consistent with the formation of multimeric defensin pores (mechanism 3). The all-or-none leakage observed, however, suggests that a minimum number of defensins must be present for a pore to form: vesicles with a large enough number of defensins bound to the surface will make a pore, whereas those with too few will not. The fraction of vesicles that form pores in such a case will be a sigmoidal function of the total peptide concentration, as we observe, provided that the total number of peptide dimers per vesicle is of the same order of magnitude as the number of dimers per pore, which we estimate to be 6–8 (see below). Approximately half of the POPG vesicles (300 μM) incubated with 0.7 μM HNP-2 release their contents. The system composition under these conditions is 1 dimer/850 lipids or ~120 dimers/vesicle. But, because large-aggregate formation will remove approximately half of the peptide from solution (Fig. 4), and because the defensin molecules involved in intervesicular contact sites may not be competent to form pores (see above), the effective number of HNP-2 dimers per vesicle is probably about 50 peptides/vesicle. This suggests that an adequate number of dimers is likely to be present to form pores.

The kinetics of HNP-2-induced leakage are also consistent with multimeric pore formation. Simulations indicate that the escape time of a small molecule from a vesicle through a pore is on the order of 10 ms, which is about 500-fold faster than than

the leakage half-times shown in Figure 9. This suggests that the half-times represent the time required to form pores. At low defensin concentration, the leakage half-times increase dramatically, as would be expected for the assembly of multimeric structures (Parente et al., 1990). At high concentrations, however, the half-times approach a constant value of ~2 min. Concentration-independent events, such as binding or translocation across the bilayer, may be the rate-limiting step in pore formation in this case.

The maximum pore diameter can be estimated using the results of the dextran permeability experiment (Fig. 12; Table 1), in which FD-4 is observed to leak out to a much greater extent than FD-20. FD-4 and FD-20 have hydrodynamic radii of approximately 18.5 Å and 29.5 Å, respectively (Bohrer et al., 1979). Because the dextrans are prolate ellipsoids with a small axis of approximately ~13 Å and axial ratios of 2.2 (FD-4) and 8.5 (FD-20), they can be visualized as tumbling rods ~26 Å in diameter, with lengths of about 57 and 228 Å. Even though both polymers have about the same rod diameter, the probability of FD-20 passing through the pore by reptation or some other motion will certainly be lower than for FD-4. In any case, the hydrodynamic radii and the rod diameters suggest that the upper limit of the pore diameter is on the order of 25 Å. Examination of the pore structure with fluorescently labeled Ficoll may yield a better estimate of pore diameter because the Ficolls are nearly spherical, with axial ratios of 1–2 over a wide range of molecular weights (Bohrer et al., 1979). The length of the pore must be similar to the thickness of the lipid bilayer, or ~35–40 Å (Lewis & Engelman, 1983). Pores constructed as an annulus of defensin dimers might, of course, have a range of sizes, but the maximum size is unlikely to be much greater than 25 Å based on our experiments. Given this, we can envision a pore formed from 6–8 dimers, organized as shown in Figure 13, that would be just large enough to allow the passage of a dextran molecule. This model is, of course, highly speculative. We have made no attempt to minimize interaction energies or even to avoid minor atomic overlaps in the model because it is only presented to demonstrate that a physically rational structure can be made that is consistent both with the experimental data and with the known structures of human defensins and phospholipid bilayers.

Figure 13 and Kinemages 2 and 3 show a computer-generated pore composed of 6 defensin dimers. The long axis of the flattened basket top is oriented at approximately 45° from the bilayer normal. In this model, the polar basket top lines the inner surface of a 20-Å channel. The outer surface of the pore, which faces the lipid acyl chains, is made of the predominantly hydrophobic residues of the basket bottom. We have oriented the dimers so that the arginine residues lie in 2 planes, parallel to the bilayer, with the α-carbons separated by ~15 Å (see Kinemage 3). Consequently, the maximum separation of the 2 planes of guanidino groups, at the ends of the arginine side chains, is approximately 25–27 Å. The arginine planes are visible in View 1 of Kinemage 3, which shows the defensin pore from the plane of the bilayer (turn the backbone off for better clarity). This is almost enough to span the phosphate-phosphate distance of a fully hydrated bilayer of ~35 Å (Lewis & Engelman, 1983). The thickness of the bilayer hydrocarbon region is between 1/2 and 3/4 of the total thickness (Lewis & Engelman, 1983; Wiener & White, 1992), or ~18–25 Å. This is somewhat smaller than the 15-Å thickness of the hydrophobic region of the pore. However, studies of gramicidin A channels (Hladky & Haydon, 1972) suggest that bilayer thickness adapts to channel length, and a similar situation would not be unreasonable for the defensin pore.

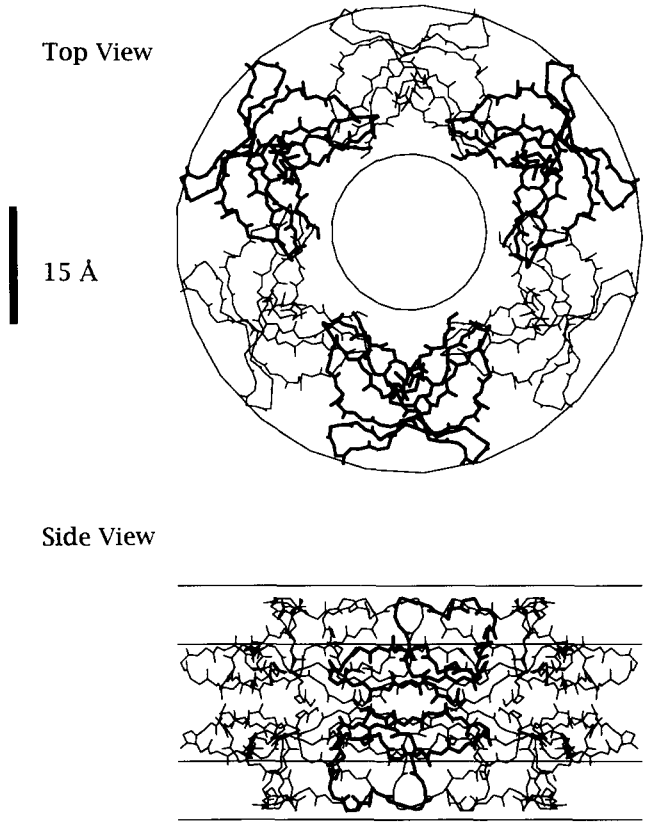

Fig. 13. Top and side views of a speculative model of a defensin pore. This image of a pore was prepared from kinemage files using the program kinplot (see Materials and methods and the Diskette Appendix). The pore is composed of 6 defensin dimers arranged with the polar basket tops (Fig. 1) lining a ~20-Å pore. The model was constructed by requiring the hydrophobic basket bottoms to face outward toward the bilayer hydrocarbon region and the arginine residues to form 2 planes parallel with the bilayer surface facing the aqueous phase (see also Kinemage 2). Single dimers are shown in bold for clarity.

The formation of defensin pores requires that multiple charged groups be transported across the bilayer, and access to bacterial inner membranes requires that defensins, despite their high charge, must be transported across the outer membrane. Ordinarily, this process would be considered energetically prohibitive (Jacobs & White, 1989), but it is possible that the amphipathic nature of the defensin dimer, as it initially interacts with anionic bilayer surfaces, may lead to the disruption of bilayer packing or the formation of nonbilayer phase lesions in the membrane, which might then decrease the barrier to charge movement across the bilayer. This idea has been proposed to explain the signal-peptide-mediated movement of proteins across bilayers (Killian et al., 1990). Defensins might also transit a membrane by passing through their own channel, which would clearly provide easier access to the inner membrane of gram-negative bacteria. The dimer of HNP-3 has dimensions of 26 × 15 × 15 Å (Hill et al., 1991) and thus could, in principle, pass through the channel we have proposed.

Conclusion

We have presented evidence that human defensin HNP-2 forms multimeric pores in lipid bilayers and proposed a model for the putative channel composed of 6–8 bilayer-spanning defensin dimers in the form of an annulus around an aqueous channel about 25 Å in diameter. This model is consistent with mechanism 3 of defensin permeabilization of membranes proposed by Hill et al. (1991). However, as pointed out by those authors, all 3 proposed modes of interaction could be involved in the activity of defensins. For instance, the initial interaction of defensins with cell membranes probably involves single dimers binding electrostatically to the cell surface (mechanism 1), which might be followed by formation of dimers of dimers (mechanism 2) and then higher multimers (mechanism 3). This is consistent with the observation that defensins induce bacteria to leak small ions (such as K^+) first, followed later by the release of larger molecules (Lehrer et al., 1989).

Ideas about the structure of transmembrane proteins, and particularly ion channels, have been dominated for 2 decades by the "helical bundle" motif since the first low-resolution structure of bacteriorhodopsin was determined by Henderson and Unwin (1975). Recently, however, nonhelical channel-forming polypeptides have also been described, including the bacterial-pore protein porin (Weiss et al., 1991) and the human tumor necrosis factor (TNF)-α (Jones et al., 1992; Kagan et al., 1992). Porin consists of trimers of β-barrels that form pores. Other examples of small, channel-forming antimicrobial peptides that, like the defensins, are rigid, cross-linked peptides rich in sheet structure include the bacterial antibiotic duramycin (Sheth et al., 1992) and the family of insect "defensins" or sapecins (Cociancich et al., 1993a). Understanding the insertion and assembly of these nonhelical, channel-forming peptides should improve our understanding of membrane protein insertion and translocation in general.

Materials and methods

Purification of human defensins

The human defensin HNP-2 was purified from human polymorphological neutrophil granules. The granules were repetitively extracted with 5% acetic acid at 0 °C. The combined extracts, containing approximately 60 mg total HNP-1, -2, and -3 were lyophilized and suspended in 5% acetic acid. The defensins were separated using a 5 × 150-cm Biogel P60 column run in 5% acetic acid at 8 °C. The defensins eluted ~0.5 L after the included volume because of interactions with the P60 matrix, and contained approximately 70% HNP-1, -2, and -3 and 30% defensin-like proteins. Final purification of HNP-1, -2, and -3 was obtained with a combination of reverse-phase and ion exchange HPLC. RP-HPLC was done using a 1 × 25-cm MICROSORB C18 column (Rainin Instrument Co., Woburn, Massachusetts) and IEX-HPLC was done with a 0.46 × 20-cm polyaspartamide cation exchange column (PolyLC Inc.). In both cases, water/acetonitrile/NH_4-acetate buffers were used. Purity of the final products was greater than 98% as judged by IEX- and RP-HPLC, acid/urea gel profiles, and amino acid analysis. Stock solutions of 30 μM in buffer were prepared weekly and used in all of the experiments.

Materials

All lipids were obtained from Avanti polar lipids (Birmingham, Alabama). Fluorescein-labeled dextrans FD-4 and FD-20 were obtained from Sigma (St. Louis, Missouri). ANTS and DPX were obtained from Molecular Probes (Eugene, Oregon). Water was glass-distilled. Except where noted, the buffer composition was 10 mM HEPES, 50 mM KCl, 1 mM EDTA, 3 mM NaN_3, pH 7.0.

Vesicle preparation

LUV of approximately 0.1 μm diameter were formed by extrusion under N_2 pressure through Nucleopore polycarbonate membranes (Mayer et al., 1986). POPC and POPG were mixed in chloroform and the solution dried under a stream of N_2. To ensure uniform vesicle composition for 2-component vesicles, the dried lipids were redissolved in cyclohexane, rapidly frozen in liquid nitrogen, and lyophilized overnight. Buffer was added to the dried lipids and the suspension was frozen and thawed 5 times prior to extrusion.

To prepare LUV with entrapped solutes (sucrose, ANTS, DPX, FD-4, and FD-20), the lipid was suspended in buffer containing the solute and was then frozen and thawed 20 times prior to extrusion and several times during the extrusion process. Lipid solutions were prepared at 50–100 mM to maximize entrapment. Approximately 10–20% of a solute is entrapped under these conditions. Solute concentrations used were 5 or 25 mM ANTS and DPX, 8 mg/mL FD-4, and 20 mg/mL FD-20. The total KCl concentration in ANTS- and DPX-containing vesicles was adjusted such that the entrapped solutions had the same osmolarity as the external 50 mM KCl buffer.

Unencapsulated ANTS and DPX were separated from encapsulated material using Sephadex G-100 packed in a 2.5-mL pasteur pipette. Untrapped FD-4 and FD-20 were removed by gel filtration using Sephadex G-100 packed into a 45 × 1.3-cm glass column run at approximately 1 mL/min. Vesicles eluted in the void volume (~11 mL) and FD-4 and FD-20 eluted at 27 mL and 17 mL, respectively. No detectable leakage of any solutes, in the absence of defensin, occurred for at least 1 week after vesicle preparation. POPG LUV made in the presence of 25 mM ANTS and DPX were unstable and reformed large vesicles within 24 h if entrapped material was not removed by gel filtration immediately after extrusion. However, after removal of external ANTS and DPX, the vesicles were stable for at least 1 week.

Fluorescence spectroscopy

Fluorescence spectroscopy was performed with a SPEX fluorolog fluorimeter that was upgraded and interfaced to a computer by OLIS Inc. (Jefferson, Georgia). All samples were in unstirred 1 × 0.4-cm quartz cuvettes masked down to a sample volume of 0.45 mL. Slits were 10 nm. Excitation and emission wavelengths were as follows: ANTS ex: 468, em: 515; NBD-PE ex: 368, em: 517; FD-4, FD-20: ex: 495, em: 518. The contribution of light scattering was negligible in all cases.

Binding and aggregation

Binding of HNP-2 to POPC/POPG vesicles was assayed by equilibrium dialysis and quantitative RP-HPLC (Wimley &

White, 1993a). Equilibrium dialysis was done using Spectrum dialysis cells with half-cell volumes of 1.5 mL. Spectrapor 4 dialysis membranes (molecular weight cutoff 12,000–14,000 Da) were used. Experiments were begun with 1 or 10 mM vesicles in one cell and 14.5 μM HNP-2 in the other. Equilibration occurred in approximately 4 h, and the dialysis was run overnight at ambient temperature (23 °C). HNP-2 was assayed by HPLC (Wimley & White, 1993a). The percent HNP-2 free is given by the ratio of the HNP-2 concentration in the buffer half-cell to the concentration in the lipid half-cell.

The fraction of HNP-2 and POPG in large aggregates (Figs. 3, 4) was assayed by measuring the total concentration of HNP-2 or POPG and the concentrations remaining in solution after centrifugation of the lipid/defensin mixtures in a tabletop centrifuge (1,000 × g) for 10 min. HNP-2 was assayed by HPLC (Wimley & White, 1993a), and POPG vesicle concentration was assayed by fluorescence using POPG vesicles doped with either 0.1 mol % NBD-PE or 0.5% diphenylhexatriene, which gave similar results.

Fusion

POPG LUV containing 1 mol each NBD-PE and rho-PE were diluted 10-fold with unlabeled POPG vesicles. No spontaneous fusion or lipid exchange was detectable for at least several days. Fusion experiments were carried out at 300 μM total vesicle concentration in a fluorescence cuvette. Defensins were added to this solution from a concentrated stock solution.

Fusion was assayed by fluorescence. Solubilization of POPG/NBD-PE/rho-PE vesicles by 0.2% Triton X-100 eliminates quenching but decreases the inherent fluorescence of NBD-PE by a factor of 1.75. Fractional fluorescence f_F is expressed as

$$f_F = (F_{final} - F_{initial})/(F_{max} - F_{initial}),$$

where F_{final} is the plateau level of fluorescence, $F_{initial}$ is the initial quenched fluorescence, and F_{max} is the maximum fluorescence expected if the rho-PE were completely diluted by the unlabeled vesicles. F_{max} is given by

$$F_{max} = 1.75 Q_{dil} \cdot F_{lys},$$

where F_{lys} is the fluorescence of Triton X-100-lysed vesicles and Q_{dil} is the expected quenching factor ($F_{quenched}/F_{unquenched}$) for the diluted rho-PE concentration, determined from a standard curve.

Contents mixing was assayed by mixing equal amounts of ANTS and DPX containing POPG LUV, at 300 μM total concentration, and monitoring ANTS fluorescence after addition of defensins. During the first 10 min after defensin addition, no detectable decrease in fluorescence was observed, indicating that contents mixing was not occurring.

Leakage of ANTS/DPX

ANTS leakage was assayed by measuring the fluorescence of ANTS in ANTS/DPX-containing vesicles (Ellens et al., 1984). ANTS and DPX were coencapsulated in POPG LUV, as described above, at 5–25 mM total concentration. The contents leakage results were independent of the ANTS/DPX concentration over this range. ANTS/DPX-containing vesicles, at 300 μM, were placed into a fluorescence cuvette and the ANTS fluorescence measured after addition of defensin. Fractional fluorescence f_F is expressed as

$$f_F = (F_{final} - F_{initial})/(F_{max} - F_{initial}),$$

where F_{final} is the plateau level of fluorescence, $F_{initial}$ is the initial quenched fluorescence, and F_{max} is the fluorescence corresponding to 100% leakage, which was measured after addition of 0.2% Triton X-100. In a separate experiment, the presence of 1 mM POPG vesicles had no effect on the quenching of externally added ANTS fluorescence by externally added DPX, indicating that DPX (an organic divalent cation) was not binding strongly to the anionic POPG.

Leakage of dextrans

Fluorescein-dextran-containing POPG LUV at 300 μM were incubated 1.5 or 5.8 μM HNP-2 for 2 h. A 100-μL sample was loaded onto a 45 × 1.3-cm Sephadex G-100 gel filtration column and 0.475-mL fractions were collected. The relative concentration of dextran in each fraction was assayed by fluorescence spectroscopy.

Preparation of graphical images from kinemage files

A pascal program for converting kinemage views into data files that can be loaded into spreadsheet programs for graphical image presentations was compiled for Microsoft® DOS execution. Examples are shown in Figures 1 and 13. The program kinplot.exe is included in the CODE directory of the Diskette Appendix. See the companion file kinplot.txt for a description.

Acknowledgments

This research was supported in part by grants from the NSF (DMB-880743) and the NIH (GM 46823) awarded to S.H.W. and from the NIH (AI 22931 and AI 31692) awarded to M.E.S. W.C.W. is supported by NIH NRSA (GM 14178). We thank David Richardson for his advice on the development of kinplot.

References

Bohrer MP, Deen WM, Robertson CR, Troy JL, Brenner BM. 1979. Influence of molecular configuration on the passage of macromolecules across the glomerular capillary wall. *J Gen Physiol 74*:583–593.

Burgess SW, Massenburg D, Yates J, Lentz BR. 1991. Poly(ethylene glycol)-induced lipid mixing but not fusion between synthetic phosphatidylcholine large unilamellar vesicles. *Biochemistry 30*:4 193–200.

Cociancich S, Ghazi A, Hetru C, Hoffmann JA, Letellier L. 1993a. Insect defensin, an inducible antibacterial peptide, forms voltage-dependent channels in *Micrococcus luteus*. *J Biol Chem 268*:19239–19245.

Cociancich S, Goyffon M, Bontems F, Bulet P, Bouet F, Menez A, Hoffmann J. 1993b. Purification and characterization of a scorpion defensin, a 4 kDa antibacterial peptide presenting structural similarities with insect defensins and scorpion toxins. *Biochem Biophys Res Commun 194*:17–22.

Cruciani RA, Barker JL, Durell SR, Raghunathan G, Guy HR, Zasloff M, Stanley EF. 1992. Magainin 2, a natural antibiotic from frog skin, forms ion channels in lipid bilayer membranes. *Eur J Pharm 226*:287–296.

Diamond G, Zasloff M, Eck H, Brasseur M, Maloy WL, Bevins CL. 1991. Tracheal antimicrobial peptide, a cysteine-rich peptide from mammalian tracheal mucosa: Peptide isolation and cloning of a cDNA. *Proc Natl Acad Sci USA 88*:3952–3956.

Eisenhauer PB, Harwig SSL, Szklarek D, Ganz T, Selsted ME, Lehrer RI. 1989. Purification and antimicrobial properties of three defensins from rat neutrophils. *Infect Immunol 57*:2021–2027.

Ellens H, Bentz J, Szoka FC. 1984. pH-induced destabilization of phosphatidylethanolamine-containing liposomes: Role of bilayer contact. *Biochemistry 23*:1532–1538.

Feigenson GW. 1989. Calcium ion binding between lipid bilayers: The four-component system of phosphatidylserine, phosphatidylcholine, calcium chloride, and water. *Biochemistry 28*:1270–1278.

Fujii G, Selsted ME, Eisenberg D. 1993. Defensins promote fusion and lysis of negatively charged vesicles. *Protein Sci 2*:1301–1312.

Grant E Jr, Beeler TJ, Taylor KM, Gable K, Roseman MA. 1992. Mechanism of magainin 2a induced permeabilization of phospholipid vesicles. *Biochemistry 31*:9912–9918.

Henderson R, Unwin PN. 1975. Three-dimensional model of purple membrane obtained by electron microscopy. *Nature 257*:28–32.

Hill CP, Yee J, Selsted ME, Eisenberg D. 1991. Crystal structure of defensin HNP3, an amphiphilic dimer: Mechanisms of membrane permeabilization. *Science 251*:1481–1485.

Hladky SB, Haydon DA. 1972. Ion transfer across lipid membranes in the presence of gramacidin A. I. Studies of the unit conduction channel. *Biochim Biophys Acta 274*:294–312.

Jacobs RE, White SH. 1989. The nature of the hydrophobic binding of small peptides at the bilayer interface: Implications for the insertion of transbilayer helices. *Biochemistry 28*:3421–3437.

Jones DE, Bevins CL. 1992. Paneth cells of the human small intestine express an antimicrobial peptide gene. *J Biol Chem 267*:23216–23225.

Jones DE, Bevins CL. 1993. Defensin-6 mRNA in human Paneth cells: Implications for antimicrobial peptides in host defense of the human bowel. *FEBS Lett 315*:187–192.

Jones EY, Stuart DI, Walker NP. 1992. Crystal structure of TNF. *Immunol Ser 56*:93–127.

Kagan BL, Baldwin RL, Munoz D, Wisnieski BJ. 1992. Formation of ion-permeable channels by tumor necrosis factor-alpha. *Science 255*:1427–1430.

Kagan BL, Selsted ME, Ganz T, Lehrer RI. 1990. Antimicrobial defensin peptides form voltage-dependent ion-permeable channels in planar lipid bilayer membranes. *Proc Natl Acad Sci USA 87*:210–214.

Killian JA, de Jong AM, Bijvelt J, Verkleij AJ, de Kruijff B. 1990. Induction of non-bilayer lipid structures by functional signal peptides. *EMBO J 9*:815–819.

Kim J, Mosior M, Chung LA, Wu H, McLaughlin S. 1991. Binding of peptides with basic residues to membranes containing acidic phospholipids. *Biophys J 60*:135–148.

LaLonde G, McDonald TV, Gardner P, O'Hanley PD. 1989. Identification of a hemolysin from *Actinobacillus pleuropneumoniae* and characterization of its channel properties in planar phospholipid bilayers. *J Biol Chem 264*:13559–13564.

Lambert J, Keppi E, Dimarcq JL, Wicker C, Reichhart JM, Dunbar B, Lepage P, Van Dorsselaer A, Hoffmann J, Fothergill J. 1989. Insect immunity: Isolation from immune blood of the dipteran *Phormia terranovae* of two insect antibacterial peptides with sequence homology to rabbit lung macrophage bactericidal peptides. *Proc Natl Acad Sci USA 86*:262–266.

Lee JY, Boman A, Sun CX, Andersson M, Jornvall H, Mutt V, Boman HG. 1989. Antibacterial peptides from pig intestine: Isolation of a mammalian cecropin. *Proc Natl Acad Sci USA 86*:9159–9162.

Lehrer RI, Barton A, Daher KA, Harwig SSL, Ganz T, Selsted ME. 1989. Interactions of human defensins with *Escherichia coli*. Mechanism of bactericidal activity. *J Clin Invest 84*:553–561.

Lehrer RI, Ganz T, Selsted ME. 1991. Defensins: Endogenous antibiotic peptides of animal cells. *Cell 64*:229–230.

Leippe M, Tannich E, Nickel R, van der Goot G, Pattus F, Horstmann RD, Muller-Eberhard HJ. 1992. Primary and secondary structure of the pore-forming peptide of pathogenic *Entamoeba histolytica*. *EMBO J 11*:3501–3506.

Leventis R, Gagne J, Fuller N, Rand RP, Silvius JR. 1986. Divalent cation induced fusion and lipid lateral segregation in phosphatidylcholine-phosphatidic acid vesicles. *Biochemistry 25*:6978–6987.

Lewis BA, Engelman DM. 1983. Lipid bilayer thickness varies linearly with acyl chain length in fluid phosphatidylcholine vesicles. *J Mol Biol 166*:211–217.

Lichtenstein A, Ganz T, Selsted ME, Lehrer RI. 1986. In vitro tumor cell cytolysis mediated by peptide defensins of human and rabbit granulocytes. *Blood 68*:1407–1410.

Mangel A, Leitao JM, Batel R, Zimmermann H, Muller WE, Schroder HC. 1992. Purification and characterization of a pore-forming protein from the marine sponge *Tethya lyncurium*. *Eur J Biochem 210*:499–507.

Mayer LD, Hope MJ, Cullis PR. 1986. Vesicles of variable sizes produced by a rapid extrusion procedure. *Biochim Biophys Acta 858*:161–168.

Nicolussi A, Massari S, Colonna R. 1982. Effect of lipid mixing on the permeability and fusion of saturated lecithin membranes. *Biochemistry 21*:2134–2140.

Ohta M, Ito H, Masuda K, Tanaka S, Arakawa Y, Wacharotayankun R, Kato N. 1992. Mechanisms of antibacterial action of tachyplesins and polyphemusins, a group of antimicrobial peptides isolated from horseshoe crab hemocytes. *Antimicrob Agents Chemother 36*:1460–1465.

Ostolaza H, Bartolomé B, Ortiz de Zárate I, de la Cruz F, Goñi F. 1993. Release of lipid vesicle contents by the bacterial protein toxin α-haemolysin. *Biochim Biophys Acta 1147*:81–88.

Pattus F, Massotte D, Wilmsen HU, Lakey J, Tsernoglou D, Tucker A, Parker MW. 1990. Colicins: Prokaryotic killer-pores. *Experientia 46*:180–192.

Pardi A, Hare DR, Selsted ME, Morrison RD, Bassolino DA, Bach AC. 1988. Solution structures of the rabbit neutrophil defensin NP-5. *J Mol Biol 201*:625–636.

Pardi A, Zhang XL, Selsted ME, Skalicky JJ, Yip PF. 1992. NMR studies of defensin antimicrobial peptides. 2. Three-dimensional structures of rabbit NP-2 and human HNP-1. *Biochemistry 31*:11357–11364.

Parente RA, Nir S, Szoka FC Jr. 1990. Mechanism of leakage of phospholipid vesicle contents induced by the peptide GALA. *Biochemistry 29*:8720–8728.

Schwarz G, Zong RT, Popescu T. 1992. Kinetics of melittin induced pore formation in the membrane of lipid vesicles. *Biochim Biophys Acta 1110*:97–104.

Selsted ME, Brown DM, DeLange RJ, Harwig SSL, Lehrer RI. 1985a. Primary structures of six antimicrobial peptides of rabbit peritoneal neutrophils. *J Biol Chem 260*:4579–4584.

Selsted ME, Harwig SSL. 1987. Purification, primary structure, and antimicrobial activities of a guinea pig neutrophil defensin. *Infect Immunol 55*:2281–2286.

Selsted ME, Harwig SSL, Ganz T, Schilling JW, Lehrer RI. 1985b. Primary structures of three human neutrophil defensins. *J Clin Invest 76*:1436–1439.

Selsted ME, Miller SI, Henschen AH, Ouellette AJ. 1992. Enteric defensins: Antibiotic peptide components of intestinal host defense. *J Cell Biol 118*:929–936.

Selsted ME, Tang YQ, Morris WL, McGuire PA, Novotny MJ, Smith W, Henschen AH, Cullor JS. 1993. Purification, primary structures, and antibacterial activities of beta-defensins, a new family of antimicrobial peptides from bovine neutrophils. *J Biol Chem 268*:6641–6648.

Shai Y, Fox J, Caratsch C, Shih YL, Edwards C, Lazarovici P. 1988. Sequencing and synthesis of pardaxin, a polypeptide from the Red Sea Moses sole with ionophore activity. *FEBS Lett 242*:161–166.

Sheth TR, Henderson RM, Hladky SB, Cuthbert AW. 1992. Ion channel formation by duramycin. *Biochim Biophys Acta 1107*:179–185.

Siegel DP. 1993. Modeling protein-induced fusion mechanisms: Insights from the relative stability of lipidic structures. In: Bentz J, ed. *Viral fusion mechanisms*. Boca Raton, Florida: CRC Press. pp 475–512.

Struck DK, Hoekstra D, Pagano RE. 1981. Use of resonance energy transfer to monitor membrane fusion. *Biochemistry 20*:4093–4099.

Tosteson MT, Tosteson DC. 1981. The sting. Melittin forms channels in lipid bilayers. *Biophys J 36*:109–116.

Wang MS, Yuan J, Yount NY, Hsieh M, Oulette AJ, Selsted ME. 1993. Rat cryptdin-1, a unique defensin isolated from rat small intestine. *Protein Sci 2*(Suppl 1):161.

Weiss MS, Abele U, Weckesser J, Welte W, Schiltz E, Schulz GE. 1991. Molecular architecture and electrostatic properties of a bacterial porin. *Science 254*:1627–1630.

White SH, Wimley WC. 1994. Peptides in lipid bilayers: Structural and thermodynamic basis for partitioning and folding. *Curr Opin Struct Biol 4*:79–86.

Wiener MC, White SH. 1992. Structure of a fluid dioleoylphosphatidylcholine bilayer determined by joint refinement of X-ray and neutron diffraction data. III. Complete structure. *Biophys J 61*:437–447.

Wilde CG, Griffith JE, Marra MN, Snable JL, Scott RW. 1989. Purification and characterization of human neutrophil peptide 4, a novel member of the defensin family. *J Biol Chem 264*:11200–11203.

Wimley WC, White SH. 1993a. Quantitation of electrostatic and hydrophobic membrane interactions by equilibrium dialysis and reverse-phase HPLC. *Anal Biochem 213*:213–217.

Wimley WC, White SH. 1993b. Membrane partitioning: Distinguishing bilayer effects from the hydrophobic effect. *Biochemistry 32*:6307–6312.

Wimley WC, Wiener MC, White SH. 1993. Interactions between human defensins and phospholipid bilayers. *Biophys J 64*:A80.

Wong M, Anthony FH, Tillack TW, Thompson TE. 1982. Fusion of dipalmitoylphosphatidylcholine vesicles at 4 degrees C. *Biochemistry 21*:4126–4132.

Woodbury DJ, Hall JE. 1988. Role of channels in the fusion of vesicles with a planar bilayer. *Biophys J 54*:1053–1063.